



ÉCOLE NATIONALE SUPÉRIEURE DE  
TECHNIQUES AVANCÉES

MASTER THESIS

# **Study of multi-antenna terminals in the presence of close scatterers**

Enric de Mur i Prior

August 2009



*Als meus pares.  
Per fer-me sentir sempre protegit.*



# Acknowledgements

Several people have been instrumental in allowing this project to be completed. I would like to thank all of them.

I will first thank the person who gave me the opportunity of coming to the ENSTA; Professor Alain Sibille, Director of the UEI, made this possible and I will be forever grateful to him for this. I thank also him for gave me the opportunity to assist to one of his courses (with Professor Christophe Roblin) and the Seminar COST2100 which were very instructive.

I will continue thanking the people who actually made this report possible. In this case I should especially thank PhD Judson Braga who guided me during the project and provided me all the attention and knowledge I needed during these months. I would like to thank also Gilles Poncelet for his help in the lab, which I really appreciate.

I also thank my friends at ENSTA. To Amir, for being there always available and always kind wishing me the best every morning, even if it was in a language that I will never understand. Thanks again to Judson for being the only person I can talk to about football during this great FC Barcelona season. Thanks to Dani, who made this experience even bigger and more enriching than I would imagine. Thanks to Francesco for his sense of humor, which I'll never forget. Thanks to Natalia, for being the kindest person at ENSTA who always was there looking after all of us.

Especially one paragraph dedicated to my friends at Supélec. I am sorry you have to live in the countryside; Paris is amazing! But thank you anyway for all the

great moments we lived together.

I want also to remember the people who helped me in different ways during all my degree. I sincerely thank my friends from Barcelona. You are too many for naming each one of you, so this is for you if you consider yourself as part of Atrapaos. I also have in mind my friends from Tarragona; Hug, Gerard and, of course, Sol who has been so important in my life.

And for the end, I leave some of the best; the people who helped me during the hard times. Especially thanks to Irene, for sharing this experience and making Paris much better; I will never forget that Paris has now something different. Thank you to all my family; my grandmother, my parents and my brother, my aunts and uncles and all my cousins.

# Abstract

Multi-antenna technologies may offer significant increases in data throughput and link range without additional bandwidth or transmit power by using spatial diversity concept. However, the radiation proprieties and return loss of these antennas as well as the channel capacity may be modified by many factors such as close scatterers (human body), mutual coupling, PCB housing, etc.

The goal of this study is to characterize the behavior of some multi-antenna prototypes in the presence of these perturbation sources. Most of the antennas are designed to work for 2.4/5.2/5.8 GHz WLAN bands and 2.5/3.5/5.5GHz WiMAX bands and are printed on PCBs of size 114x64 mm<sup>2</sup> which follow the average dimensions of PDAs found in the market.

Different antennas were designed, simulated and fabricated. In Chapter 4 the results for the circular monopole array antenna is widely detailed. In the Appendix, designs of other antennas simulated and/or fabricated are shown.





# Contents

Acknowledgements.....	i
Abstract .....	iii
Contents .....	v
Chapter 1. Introduction.....	1
1.1 Data Multiplexing.....	2
1.1.1 Spatial Multiplexing of data .....	3
1.2 Adaptative beamformer.....	6
1.3 Multidirectional beam patterns.....	6
1.4 Abstract of recent works on antenna modeling in the presence of close scatterers .....	7
Chapter 2. Antenna Basics .....	13
2.1 Antenna radiation.....	13
2.2 Gain.....	14
2.3 Directivity.....	16
2.4 Path loss .....	17
2.5 Scattering Parameters .....	18

Chapter 3. Measurements campaigns.....	21
3.1 Hand phantom measurements.....	22
3.1.1 Measurements.....	25
3.2 On-body Hand measurements.....	28
3.2.1 Measurements.....	28
3.3 SAM head phantom.....	30
3.3.1 Measurements.....	31
Chapter 4. Design and manufacturing of new UWB devices.....	35
4.1 Simulations .....	35
4.2 Measurements.....	40
4.3 Conclusion .....	43
Appendix.....	45
ANTENNAS.....	45
PIFA ANTENNA .....	47
SIMULATIONS.....	48
Bibliography .....	49

# Chapter 1. Introduction

Modern mobile communication terminals such as cell phones and PDAs attempt to guarantee multimedia services at a high data rate such as internet, online shopping, video telephones, etc. Consequently, new challenges for the improvement of the communication link emerge, including interference and transmitted energy reduction, and increased range and capacity. In upcoming years, smart antennas, such as beamforming and MIMO/SIMO systems, will be massively employed as a high-performance solution to these challenges [1].

Beamforming used for SDMA multiplexing access is a powerful technique for user discrimination in space domain, and MIMO/SIMO systems considerably increase the channel capacity when the ports associated to different radiating elements are sufficiently uncorrelated.

The successful implementation of such systems implies detailed knowledge on the mobile propagation channel. The Propagation modeling (or characterization) is important because it shows how the electromagnetic waves propagate in a given type of environment. Statistical models give some parameters that allow the understanding of the channel behavior in average, and its variability.

From the moment you know how the propagation channel behaves, you can better design communication systems, calculate channel capacity (maximum allowed data rate), and design wireless networks (RF planning).

Mostly of statistical models don't take into account some scatterers which are close to the mobile terminals such as the user's hand and head. These scatterers

may change the return loss and far-field radiation properties of the terminal. When associated to the antenna radiation pattern, the complete channel model seems less realistic if this close scatterers influence is not taken into account.

In the case of a multiport system the Kronecker approach allows the propagation channel to decouple effectively the receiver and the transmitter, permitting a separate characterization of the propagation channel, transmitting and receiving branches.

The goal of this study is to provide “antenna plus close scatterers” measurements that can be used in future works for channel modeling. In chapter I, basic concepts of spatial multiplexing using adaptative beamformer and multiport systems such as MIMO are introduced. Also in chapter I, a brief abstract of recent works on antenna measurements and simulations in presence of close scatterers is presented. In Chapter II, the basic concepts of antennas are presented since antenna measurements are the scope of interest in this study. Chapter III shows the measurement setups and results for different terminals and configurations. This work ends in the Chapter IV with a brief conclusion.

## 1.1 Data Multiplexing

Multiplexing is a process where multiple analog message signals or digital data streams are combined into one signal over a shared medium. The aim is to share an expensive resource. For example, in telecommunications, several phone calls may be transferred using one wire. It originated in telegraphy, and is now widely applied in communications.

The multiplexed signal is transmitted over a communication channel, which may be a physical transmission medium. The multiplexing divides the capacity of the low-level communication channel into several higher-level logical channels, one for each message signal or data stream to be transferred. A reverse process, known as demultiplexing, can extract the original channels on the receiver side.

A device that performs the multiplexing is called a multiplexer (MUX), and a

device that performs the reverse process is called a demultiplexer (DEMUX). Inverse multiplexing (IMUX) has the opposite aim as multiplexing, namely to break one data stream into several streams, transfer them simultaneously over several communication channels, and recreate the original data stream.

Many strategies of multiplexing exist according to the used communication protocol that can combine them to reach the most efficient use; the best known are:

- The multiplexing by division of time or TDM (Time division multiplexing);
- The multiplexing by division of frequency or FDM (Frequency-division multiplexing) and his equivalent in optical communications, by division of WDM or wavelength (of Wavelength);
- The multiplexing by division in code or CDM (Code division multiplexing).
- The multiplexing by spatial division (Spatial Multiplexing, often abbreviated as SM or SMX).

Spatial multiplexing is a transmission technique in MIMO wireless communication to transmit independent and separately encoded data signals, so called streams, from each of the multiple transmits antennas. Therefore, the space dimension is reused, or multiplexed, more than one time.

### 1.1.1 Spatial Multiplexing of data

Antenna diversity, also known as space diversity, is any one of several wireless diversity schemes that use two or more antennas to improve the quality and reliability of a wireless link [2]. Often, especially in urban and indoor environments, there is not a clear line-of-sight (LOS) between transmitter and receiver. Instead the signal is reflected along multiple paths before finally being received. Each of these bounces can introduce phase shifts, time delays, attenuations, and even distortions that can destructively interfere with one

another at the aperture of the receiving antenna. Antenna diversity is especially effective at mitigating these multipath situations. This is because multiple antennas afford a receiver several observations of the same signal. Each antenna will experience a different interference environment. Thus, if one antenna is experiencing a deep fade, it is likely that another has a sufficient signal. Collectively such a system can provide a robust link. While this is primarily seen in receiving systems (diversity reception), the analog has also proven valuable for transmitting systems (transmit diversity) as well.

Inherently an antenna diversity scheme requires additional hardware and integration versus a single antenna system but due to the commonality of the signal paths a fair amount of circuitry can be shared. Also with the multiple signals there is a greater processing demand placed on the receiver, which can lead to tighter design requirements. Typically, however, signal reliability is paramount and using multiple antennas is an effective way to decrease the number of drop-outs and lost connections.

Antenna diversity [3] can be realized in several ways. Depending on the environment and the expected interference, designers can employ one or more of these methods to improve signal quality. In fact multiple methods are frequently used to further increase reliability.

- Spatial Diversity.
- Pattern Diversity.
- Polarization Diversity.
- Adaptive Arrays.

Spatial diversity employs multiple antennas, usually with the same characteristics, that are physically separated from one another. Depending upon the expected incidence of the incoming signal, sometimes a space on the order of half a wavelength is sufficient, or even less.

In radio, multiple-input and multiple-output, or MIMO, is the use of multiple antennas at both the transmitter and receiver to improve communication

performance. It is one of several forms of smart antenna technology.

MIMO technology [4] has attracted enormous attention in wireless communications, since it offers significant increases in data throughput and link range without additional bandwidth or transmit power. It achieves this by higher spectral efficiency (more bits per second per hertz of bandwidth) and link reliability or diversity (reduced fading). Because of these properties, MIMO is a current theme of international wireless research.

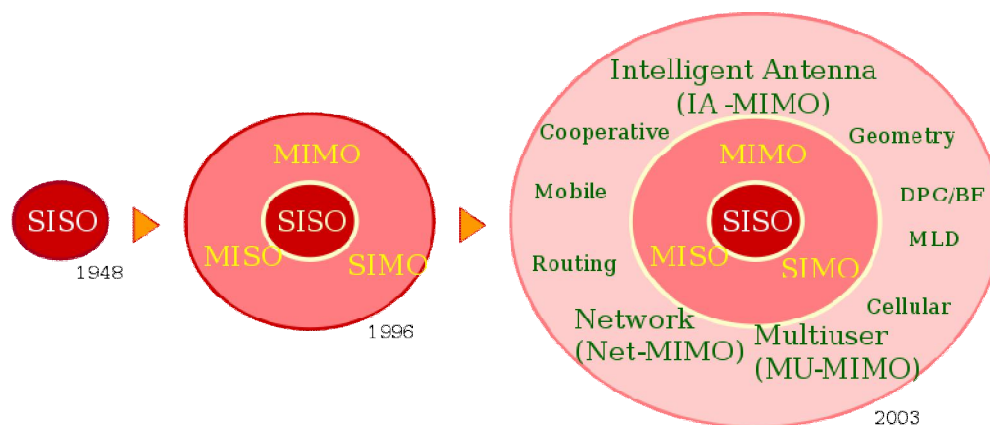


Figure 1

## Forms of MIMO

SIMO (single input, multiple output) in which multiple antennas are used at the destination (receiver).

MISO (multiple input, single output) in which multiple antennas are used at the source (transmitter).

MIMO (multiple input, multiple output) in which multiple antennas are used at both the source (transmitter) and the destination (receiver).

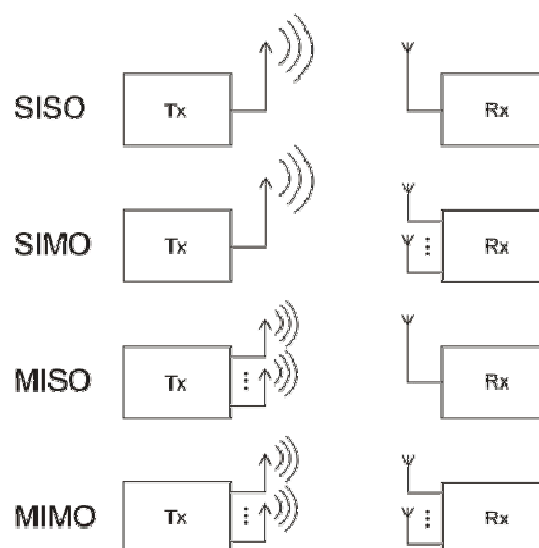


Figure 2

## 1.2 Adaptative beamformer

A special case in which spatial diversity is used is in phased antenna arrays that can be used for beamforming. Beamforming [5] is a signal processing technique used in sensor arrays for directional signal transmission or reception. This spatial selectivity is achieved by using adaptive or fixed receive/transmit beam patterns. The improvement compared with an omnidirectional reception/transmission is known as the receive/transmit gain (or loss).

Beamforming can be used for either radio or sound waves. It has found numerous applications in radar, sonar, seismology, wireless communications, radio astronomy, speech, and biomedicine. Adaptive beamforming is used to detect and estimate the signal-of-interest at the output of a sensor array by means of data-adaptive spatial filtering and interference rejection.

An adaptive beamformer is a beamforming system which performs adaptive spatial signal processing with an array of radar antennas (or phased array) in order to transmit or receive signals in different directions without having to mechanically steer the array. The main distinction between an adaptive beamformer and a conventional beamforming system is the ability of the former to adjust its performance to suit differences in its environment. A particularly important feature, in military applications, is the potential for an adaptive beamformer to reduce sensitivity to certain directions of arrival so as to counteract jamming by hostile transmissions.

If the beamforming is performed digitally in baseband, a system of user multiplexing in Space Domain (SDMA) may be used. The data associated to each user may be recovered using antenna array weights calculated through the user's direction.

## 1.3 Multidirectional beam patterns

A multiport antenna system may provide multidirectional beam patterns with



minimum interference comprising multiple, as for example a multiport antenna contains two types of radiating elements mounted adjacently. The first elemental antenna is responsive to energy having a first polarization, while the second elemental antenna is responsive to energy having a polarization orthogonal to the first polarization. With such an arrangement, all the radiating elements are located in close proximity without coupling signals to each other, and each element is capable of producing a directional radiation pattern in an independent manner. Consequently, the physical area required to install the antenna is minimized, and the antenna provides very good hemispherical coverage and for example may be placed anywhere on the ceiling of a room to provide coverage of the entire space.

## 1.4 Abstract of recent works on antenna modeling in the presence of close scatterers

Many researchers have been working on antenna modeling in the last years and on the effect of close scatterers on the radiation and matching behavior of the antennas and the overall system performance.

The analyses are sometimes based on measurements, simulations or both measurements (antenna properties) and simulations (channel). The choice of data acquisition technique may depend on the type of metric that is wanted, available equipments, and sometimes available human samples (volunteers) to hold the terminals.

In different works about multiantenna systems, Chiau [6] and Plicanic [7] calculated the mean effective gain, the correlation between elements and the diversity gain (usually for 1% or 50% of the CDF curve) by associating the measured radiation pattern in 3D with statistical models of angle spreading (Laplacian, Gaussian, etc).

In the works of Mellah-Sibille [8] and Gomes [9], human samples are used to hold the terminals in many different positions and generate statistical variability from a number of measurements. Statistical analyses of mutual coupling, correlation and mean matching efficiency are given.

In order to evaluate performance metrics such as MIMO capacity, correlation and diversity gain from real samples of the channel instead of using statistical models, Beach [10] performed a measurement campaign for many scenarios. Browse and Harrysson [11] used positioners at transmitter and receiver for generating a channel grid of samples using few scenarios. In these works, a human body phantom is used at the receiver as close scatterer source.

Harrysson [11] also proposed a statistical study by continuously measuring narrowband channels along the movement of the mobile station passing through many rooms in indoor environments. Thousands of samples in time, sub-bands and spatial domains were used to generate statistics of many important performance metrics such as the SIMO/MIMO channel capacity, diversity gain, antenna correlation, coherence time and coherence band.

# Chapter 2. Antenna Basics

## 2.1 Antenna radiation

Antennas radiate spherical waves that propagate in the radial direction for a coordinate system centered on the antenna [12]. At large distances, spherical waves can be approximated by plane waves. Plane waves are useful because they simplify the problem.

The Poynting vector describes both the direction of propagation and the power density of the electromagnetic wave. It is found from the vector cross product of the electric and magnetic fields and is denoted  $\mathbf{S}$ :

$$\mathbf{S} = \mathbf{E} \times \mathbf{H}^* \quad \frac{W}{m^2}$$

Root mean square (RMS) values are used to express the magnitude of the fields.  $\mathbf{H}^*$  is the complex conjugate of the magnetic field phasor. The magnetic field is proportional to the electric field in the far field. The constant of proportionality is  $\eta$ , the impedance of free space ( $\eta = 376.73\Omega$ ):

$$|\mathbf{S}| = S = \frac{|\mathbf{E}|^2}{\eta} \quad \frac{W}{m^2}$$

Because the Poynting vector is the vector product of the two fields, it is orthogonal to both fields and the triplet defines a right-handed coordinate

system: (E, H, S).

Consider a pair of concentric spheres centered on the antenna. The fields around the antenna decrease as  $1/R$ ,  $1/R^2$ ,  $1/R^3$ , and so on. Far from the antenna we consider only the radiated fields and power density. The power flow is the same through concentric spheres:

$$4\pi R_1^2 S_{1,avg} = 4\pi R_2^2 S_{2,avg}$$

The average power density is proportional to  $1/R^2$ . Consider differential areas on the two spheres at the same coordinate angles. The antenna radiates only in the radial direction; therefore, no power may travel in the  $\theta$  or  $\phi$  direction. Power travels in flux tubes between areas, and it follows that not only the average Poynting vector but also every part of the power density is proportional to  $1/R^2$ :

$$S_1 R_1^2 \sin \theta d\theta d\phi = S_2 R_2^2 \sin \theta d\theta d\phi$$

14

---

Since in a radiated wave  $S$  is proportional to  $1/R^2$ ,  $E$  is proportional to  $1/R$ . It is convenient to define radiation intensity to remove the  $1/R^2$  dependence:

$$U(\theta, \phi) = S(R, \theta, \phi) R^2 \quad W/\text{solid angle}$$

Radiation intensity depends only on the direction of radiation and remains the same at all distances. A probe antenna measures the relative radiation intensity (pattern) by moving in a circle (constant  $R$ ) around the antenna.

## 2.2 Gain

Gain is a measure of the ability of the antenna to direct the input power into radiation in a particular direction and is measured at the peak radiation intensity. Consider the power density radiated by an isotropic antenna with input power  $P_0$  at a distance  $R$ :  $S = P_0/4\pi R^2$ . An isotropic antenna radiates equally in all directions, and its radiated power density  $S$  is found by dividing the radiated power by the area of the sphere  $4\pi R^2$ . The isotropic radiator is considered to be

100% efficient. The gain of an actual antenna increases the power density in the direction of the peak radiation:

$$S = \frac{P_0 G}{4\pi R^2} = \frac{|E|^2}{\eta} \quad \text{or} \quad |E| = \frac{1}{R} \sqrt{\frac{P_0 G \eta}{4\pi}} = \sqrt{S_\eta}$$

Gain is achieved by directing the radiation away from other parts of the radiation sphere. In general, gain is defined as the gain-biased pattern of the antenna:

$$S(\theta, \phi) = \frac{P_0 G(\theta, \phi)}{4\pi R^2} \quad \text{power density}$$

$$U(\theta, \phi) = \frac{P_0 G(\theta, \phi)}{4\pi} \quad \text{radiation intensity}$$

The surface integral of the radiation intensity over the radiation sphere divided by the input power  $P_0$  is a measure of the relative power radiated by the antenna, or the antenna efficiency:

$$\frac{P_r}{P_0} = \int_0^{2\pi} \int_0^\pi \frac{G(\theta, \phi)}{4\pi} \sin\theta \, d\theta \, d\phi = \epsilon_{cd} \quad \text{efficiency}$$

---

15

where  $P_r$  is the radiated power.

In the above formula, antenna radiation efficiency only includes conduction efficiency and dielectric efficiency and does not include reflection efficiency as part of the total efficiency factor. Moreover, the IEEE standards state that "gain does not include losses arising from impedance mismatches and polarization mismatches". Antenna Absolute Gain is another definition for antenna gain. However, Absolute Gain (or effective) does include the reflection or mismatch losses [13].

$$G_{abs}(\theta, \phi) = \epsilon_{refl} G(\theta, \phi) = (1 - \Gamma^2)(G(\theta, \phi))$$

In this equation,  $\epsilon_{refl}$  is the reflection efficiency. Since the term  $\epsilon_{cd}$  includes the dielectric and conduction efficiency, the term  $\epsilon_{eff}$  is the total antenna

efficiency factor.

$$\epsilon_{eff} = \epsilon_{cd}\epsilon_{refl}$$

Mutual coupling has also to be taken into account in the antenna array performance. Mutual coupling arises due to the interaction of two or more elements being in close proximity to each other. This effect is observed during the transmission or reception of elements in the array. The effects of mutual coupling can be modeled by the use of full-wave numeric electromagnetic solvers incorporating methods such as the finite element method, finite difference time domain method and method of moments. These mutual coupling effects can be described by an impedance matrix (Z).

Therefore, the measured signal including mutual coupling effects can be given as:

$$\bar{X} = \bar{Z}(\bar{X}_d + \bar{X}_i) + \bar{X}_n$$

where  $X_d$  is the desired signal vector,  $X_i$  the interference signal vector, and  $X_n$  the thermal noise vector [21].

The effect of mutual coupling can be reduced by minimizing the interaction between elements in the array. One of the ways to achieve this is by adjusting the interelement separation.

## 2.3 Directivity

Directivity is a measure of the concentration of radiation in the direction of the maximum:

$$directivity = \frac{\text{maximum radiation intensity}}{\text{average radiation intensity}} = \frac{U_{max}}{U_0}$$

Directivity and gain differ only by the efficiency, but directivity is easily estimated from patterns. Gain—directivity times efficiency—must be measured.

The average radiation intensity can be found from a surface integral over the radiation sphere of the radiation intensity divided by  $4\pi$ , the area of the sphere in steradians:

$$\text{average radiation intensity} = \int_0^{2\pi} \int_0^\pi \frac{U(\theta, \phi)}{4\pi} \sin\theta d\theta d\phi = U_0$$

This is the radiated power divided by the area of a unit sphere. The radiation intensity  $U(\theta, \phi)$  separates into a sum of co- and cross-polarization components:

$$U_0 = \int_0^{2\pi} \int_0^\pi \frac{U_c(\theta, \phi) + U_x(\theta, \phi)}{4\pi} \sin\theta d\theta d\phi$$

Both co- and cross-polarization directivities can be defined:

$$\text{directivity}_c = \frac{U_{c,max}}{U_0} \quad \text{directivity}_x = \frac{U_{x,max}}{U_0}$$

Directivity can also be defined for an arbitrary direction  $D(\theta, \phi)$  as radiation intensity divided by the average radiation intensity, but when the coordinate angles are not specified, we calculate directivity at  $U_{max}$ .

## 2.4 Path loss

We combine the gain of the transmitting antenna with the effective area of the receiving antenna to determine delivered power and path loss. Combining the two, we obtain the path loss:

$$\frac{P_d}{P_t} = \frac{A_2 G_1(\theta, \phi)}{4\pi R^2}$$

Antenna 1 transmits, and antenna 2 receives. If the materials in the antennas are linear and isotropic, the transmitting and receiving patterns are identical (reciprocal). When we consider antenna 2 as the transmitting antenna and antenna 1 as the receiving antenna, the path loss is

$$\frac{P_d}{P_t} = \frac{A_1 G_2(\theta, \phi)}{4\pi R^2}$$

Since the responses are reciprocal, the path losses are equal and we can

gather and eliminate terms:

$$\frac{G_1}{A_1} = \frac{G_2}{A_2} = \text{constant}$$

Because the antennas were arbitrary, this quotient must equal a constant. This constant was found by considering the radiation between two large apertures:

$$\frac{G}{A} = \frac{4\pi}{\lambda^2}$$

We substitute this equation into path loss to express it in terms of the gains or effective areas:

$$\frac{P_d}{P_t} = G_1 G_2 \left( \frac{\lambda}{4\pi R} \right)^2 = \frac{A_1 A_2}{\lambda^2 R^2}$$

We make quick evaluations of path loss for various units of distance  $R$  and for frequency  $f$  in megahertz using the formula

$$\text{path loss}(dB) = K_U + 20 \log(fR) - G_1(dB) - G_2(dB)$$

where  $K_U$  depends on the length units being -27.55 for meters:

## 2.5 Scattering Parameters

Once an antenna is designed and constructed, it is essential to validate the design with proper measurements, a crucial element of the development process [14]. The most important measurement is the radiation pattern measurement.

A two-port network is shown, in which  $a_1$  and  $a_2$  are the input whilst  $b_1$  and  $b_2$  are the output at Port 1 and Port 2, respectively. This network is characterized by scattering parameters, or S-parameters:

$$[S] = \begin{bmatrix} S_{11} & S_{12} \\ S_{21} & S_{22} \end{bmatrix}$$





Figure 3

which links the input to the output by:

$$\begin{bmatrix} b_1 \\ b_2 \end{bmatrix} = \begin{bmatrix} S_{11} & S_{12} \\ S_{21} & S_{22} \end{bmatrix} \begin{bmatrix} a_1 \\ a_2 \end{bmatrix}$$

Thus, we have:

- $S_{11}$  = Port 1 reflection coefficient =  $b_1/a_1$ ;
- $S_{12}$  = Port 2 to Port 1 transmission coefficient/gain =  $b_1/a_2$ ;
- $S_{21}$  = Port 1 to Port 2 transmission coefficient/gain =  $b_2/a_1$ ;
- $S_{22}$  = Port 2 reflection coefficient =  $b_2/a_2$ .

S-parameters are actually reflection and transmission coefficients for a network of N ports. In this case, N=2. These parameters were originally introduced in optics, where optical waves were scattered by objects. The concepts were later extended to radiowaves and RF engineering, but the term 'S-parameters' has remained unchanged. It should be pointed out that if a network is passive and contains only isotropic and loss-free materials that influence the transmitted signal, the network will obey

- the reciprocity principle, which means  $S_{21} = S_{12}$  or generally  $S_{mn} = S_{nm}$
- the law of power conservation

$$[S]^H [S] = [I]$$

Where  $[S]^H$  is the complex conjugate transpose of the S-parameter matrix  $[S]$  and  $[I]$  is the identity/unit matrix. For a 2-port loss-free network, we have

$$|S_{11}|^2 + |S_{21}|^2 = 1$$

$$|S_{22}|^2 + |S_{12}|^2 = 1$$

Which is equivalent to

$$|a_1|^2 + |a_2|^2 = |b_1|^2 + |b_2|^2$$

The input power is the same as the output power, as expected. Almost all antennas, attenuators, cables, splitters and combiners are reciprocal (but maybe not loss-free) networks. We can clearly see that a transmitting-receiving antenna system in the space can be considered a 2-port network.

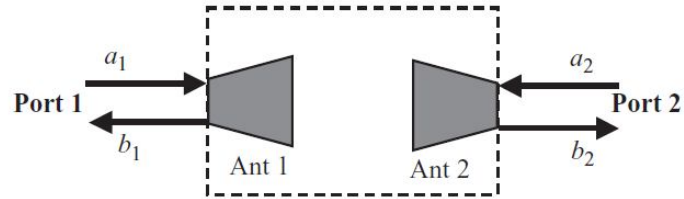


Figure 4

The transmission and reflection can be characterized using S-parameters:

- $S_{11}$  and  $S_{22}$  are the reflection coefficients of Antenna 1 and Antenna 2, respectively. They indicate how well the antenna feed line is matched with the antenna.
- $S_{21}$  and  $S_{12}$  are the transmission coefficients from one antenna to another. They are determined by the characteristics of both antennas (such as radiation patterns, matching) and the separation between them.

# Chapter 3. Measurements

## campaigns

The implementation of multiband diversity antennas in compact mobile handsets, for the purpose of increasing transmission quality, is a topic of current interest in the mobile phone industry. In order to achieve the expected performance improvement in typical operating conditions, we not only have to contend with the challenges of designing multiple multiband antennas, which are closely spaced within the compact handset and thus strongly interacting with one another electromagnetically, we also need to keep in check the electromagnetic interaction between the whole antenna system (i.e., the handset) and the user [15].

21

---

Previous studies have concluded that the presence of a user degrades the mean effective gain (MEG) of the diversity antennas significantly [16]. Different results have been presented on the effect of the user on the correlation coefficient; no effect and a significant increase of the correlation have been pointed out [17]. However, these studies have been performed on simple single band antennas in talk position. In other studies [15] further results were presented by choosing the diversity antenna system to comprise compact versions of PIFA and monopole antennas which cover three WCDMA bands: WCDMA850, WCDMA1800 and UMTS. Such compact antennas are easily conformable for small mobile phone products. The choice of the bands, as well as the evaluation of the diversity performance for the data mode position, is

derived from the increasing demand on HSDPA applications in the mobile phone market.

These studies show that for a multiband antenna approximately 5dB of diversity system gains (DSGs) can be obtained for the higher frequency bands of WCDMA1800 and UMTS when held in data mode position. For the lowest band, WCDMA850, the hand degrades the radiation performance severely, which leads to small or negligible DSGs, despite having uncorrelated branches. However, they emphasize that by definition DSG is calculated with respect to the reference case of an ideal antenna in free space with 100% efficiency. Contrary to other studies, which consider user effects in talk position, they find that in data mode position the correlation is relatively unaffected, and it is even reduced for the WCDMA850 band. The hand model affects the antenna patterns, making them more directive and orthogonal to each other for the lower band. Other evaluated performance metrics for the lowest band are, due to high coupling, much worse than those for the two higher bands. This is the consequence of restricting the size of the prototype considered to that of a typical mobile handset.

### 3.1 Hand phantom measurements

Phantom hands [18] should be integral parts in any setup for testing wireless handheld transceivers. However, the main supplier of Hand phantoms, MCL technology, decided not to include a hand phantom in the assessment of the exposure of the head to electromagnetic fields from cellular telephones. In the testing of these telephones, the device under test is placed next to a head-shaped phantom shell filled with tissue equivalent liquid; a volumetric scan of the electric field induced in the head by the device is obtained and expressed as specific absorption rate (SAR). The head phantom, known as standard anthropomorphic model (SAM), has well defined internal and external contours; indeed the whole process is strictly described in standard procedures (IEC62209-1, EN62209:2006, and IEEE1528-2003). The reasons given for not using the hand were practical difficulties in specifying a unique hand holding position that is

applicable to all devices, and with respect to SAR in the head, numerical studies suggest that not modeling the hand provides a conservative estimate. The latter is the compelling reason for not using a hand in SAR testing; the former is more of an observation because the practical problems cited are not insurmountable. Technical performance tests are made under realistic conditions, including having hand phantoms to hold the device under test as and where appropriate. SAM shells, filled with tissue equivalent liquid, are used to simulate the head (CTIA 2003), there is, however, no specified standard hand for use in these tests.

Phantom hands have been in use since the early 1990s. Hands available at that time were more elaborate than practical, made from three types of tissue: bone, muscle and skin each positioned according to the basic hand anatomy, the dielectric properties (relative permittivity  $\epsilon_r$  and conductivity  $\sigma$  of the materials matched those of the corresponding tissue in the range 900-1800MHz. They served a purpose, demonstrated the effect of the proximity of the hand on the radiation from wireless transceivers but they were rigid and had only a single open grip to accommodate the size of the large cellular telephones of the time. In the late 1990s they were replaced with hands made from homogeneous skin equivalent material as it was argued that, for all practical purposes, the absence of internal anatomy would not affect the coupling mechanism, the interaction is localized and focusing effects are negligible. The shape and size of the hand were also changed in response to feedback from users and to accommodate smaller devices but the changes were not carried out in a systematic manner or in accordance with pre-determined criteria.

The anthropometric and dielectric properties of the hand phantom are the two most important aspects to be defined; this study [18] covers the dielectric properties. They proposed target dielectric properties; and they showed that it is possible to develop materials that are physically suitable for making hand phantoms and meet the target dielectric properties.

It's been assumed that the nature of the interaction between a handheld transceiver and the hand holding it is mostly inductive in nature and greatly

affected by the dielectric properties of the tissue in closest proximity to it. On this basis it's been recommended target permittivity and conductivity values derived from the dielectric properties of the palm of the hand.

MCL fabricates Carbon-silicone hand phantoms with the following Dielectric properties of solid inner SAM material:

Frequency (MHz)	Relative permittivity, $\epsilon_r$	Conductivity, $\sigma$ (S/m)
130.0	70.5	0.27
143.8	68.3	0.29
159.0	66.3	0.30
175.9	64.4	0.32
194.5	63.0	0.34
215.1	61.5	0.37
237.9	60.1	0.40
263.1	58.5	0.42
291.0	57.0	0.45
321.8	55.5	0.48
355.9	54.2	0.51
393.6	52.8	0.54
435.4	51.4	0.57
481.5	50.1	0.61
532.5	48.9	0.65
588.9	47.7	0.70
651.3	46.5	0.74
720.4	45.3	0.79
796.7	44.3	0.83
881.1	43.4	0.88
974.5	42.6	0.94
1,077.8	41.7	1.02
1,192.0	40.6	1.10
1,318.3	39.7	1.16
1,458.0	39.0	1.23
1,612.5	38.3	1.32
1,783.3	37.6	1.43

Frequency (MHz)	Relative permittivity, $\epsilon_r$	Conductivity, $\sigma$ (S/m)
1,972.3	36.8	1.55
2,181.3	36.1	1.67
2,412.4	35.4	1.81
2,668.1	34.6	1.97
2,950.8	33.9	2.14
3,263.5	33.1	2.33
3,609.3	32.3	2.54
3,991.7	31.5	2.77
4,414.7	30.7	3.03
4,882.5	29.8	3.30
5,399.9	28.8	3.58
5,972.1	27.9	3.87
6,605.0	26.8	4.13
7,304.9	25.9	4.35
8,078.9	25.0	4.52
8,935.0	24.2	4.61
9,881.8	23.6	4.64
10,929.0	23.3	4.64

### 3.1.1 Measurements

A measurement campaign was performed with the hand phantom, using the following parameters:

Measurement equipment	VNA Rohde & Schwarz ZVA40
Band Width	400 MHz – 4 GHz
Frequency step	10 MHz (361 steps)
BW Resolution	1 KHz
Azimuth step	10° (37 steps)
Power	16 dBm
Terminal	Sagem SG4C, SG9C and Vodafone
Orientation (respect horizontal)	15°, 30° and 45°
Hand-holding position	Landscape and portrait

This is a photo of the actual scenario:

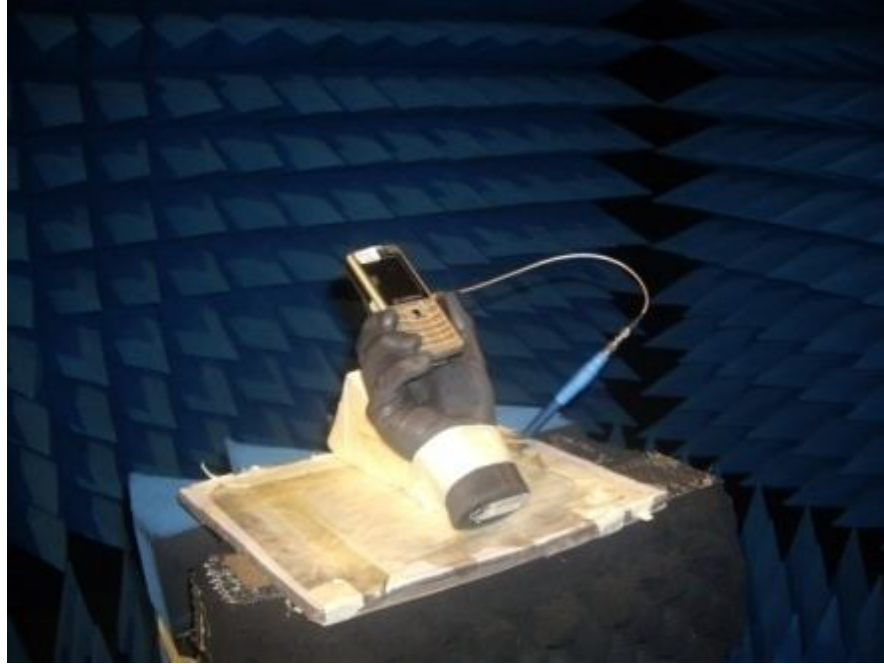


Figure 5 Actual scenario for Hand phantom measurements

The different terminals used in this measurement campaign were modified in order to access the antenna properly. SMA connectors were used to feed the antennas. This type of connector is very well-known because it's widely used in many applications as it is a very cost-effective connector and suitable for many purposes and it offers excellent electrical performance up to 18 GHz [22].



Figure 6 SMA connector

Obviously, the fact of having a cable near to the terminal is affecting the radiation pattern. Taking into account that the terminals usually have a vertical polarization (understanding vertical as the same direction of the virtual line that joints the microphone and the speaker of the terminal) and the cable is attached orthogonally to this polarization, we can assume that the effect is reduced considerably.

In this photo, portrait hand-holding position is used. Handheld portables



digital devices nowadays often include interactive multimedia capabilities. These capabilities change the way of using the portable devices such as PDAs or mobile phones. This measurement campaign is mainly focused on the use of the portable devices in other situations than the talking mode.

SG9C, freq 2.44GHz, V-pol, Or: 30°, Hand-held: portrait and landscape

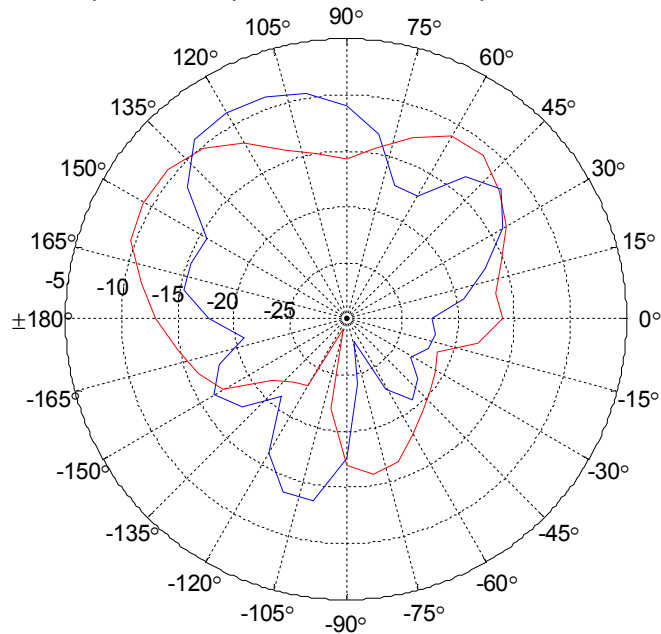


Figure 7 Measured gain in azimuth: landscape (blue), portrait (red)

The previous figure show the radiation patterns for the terminal test SG9C at freq = 2.44 GHz, at orientation = 30° comparing the two hand-holding positions: landscape (in blue) and portrait (in red).

The goal of these measurements is not to extract conclusions from the comparison between two consecutive positions (we refer to consecutive measurements as those which differs in just one parameter and just one of step of this parameter). It should be noted that the tiny variations between different positions measured may be on the order of a wavelength. Considering these scenarios, the radiation patterns of two consecutive measurements will be different, of course, but since the wavelength is on the order of the variation for some of the frequency range these differences cannot be linked directly to the parameter change.

The main goal of these measurements is to collect statistical variability by varying the position of the terminal plus phantom.

## 3.2 On-body Hand measurements

The human hand influences small terminal antennas performances, and it is the main responsible of absorption and detuning. Despite its importance in both mobile phone design and validation processes, it is still difficult to take it into account. In fact there is a lack of knowledge in the categorization of the hand grip positions of mobile phone users [20].

This campaign intends to reproduce the natural environment that is affecting the terminal. The fact that this was an on-body campaign allowed us to reproduce different scenarios such as different hand-grips (soft and firm). And of course, not only the hand will affect the terminal radiation pattern; also the body will have some effects on the measurements.

### 3.2.1 Measurements

This is a photo of the actual scenario.

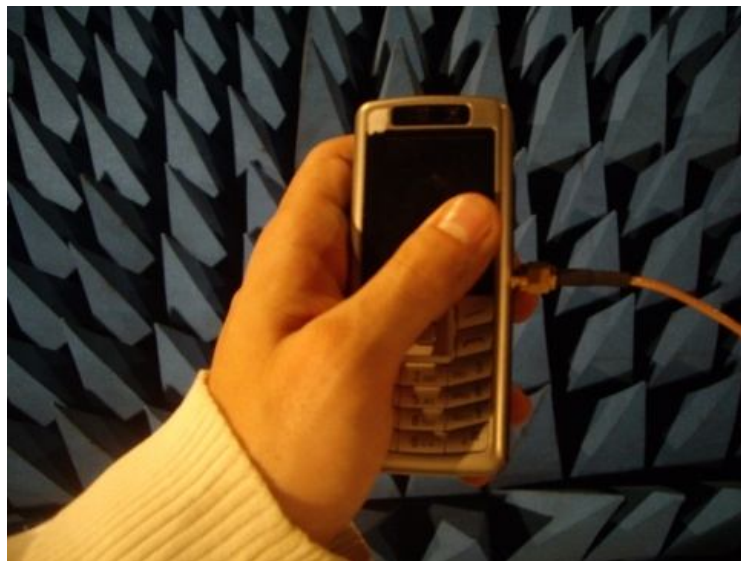


Figure 8 Actual scenario for On-body hand measurements

These are the parameters of the measurements campaign.

Measurement equipment	VNA Rohde & Schwarz ZVA40
Band Width	400 MHz – 4 GHz
Frequency step	10 MHz (361 steps)
BW Resolution	1 KHz
Azimuth step	5° (69 steps)
Power	16 dBm
Terminal	Sagem SG4C, SG9C and Vodafone
Hand-grip	Soft and firm
Hand-holding position	Landscape and portrait

The next figure show the radiation patterns for the terminal test SG9C at freq=2.44 GHz, at portrait hand-holding position comparing the two hand-grips: soft (in blue) and firm (in red). We can observe that the firm hand-grip has an attenuating influence in the radiation pattern.

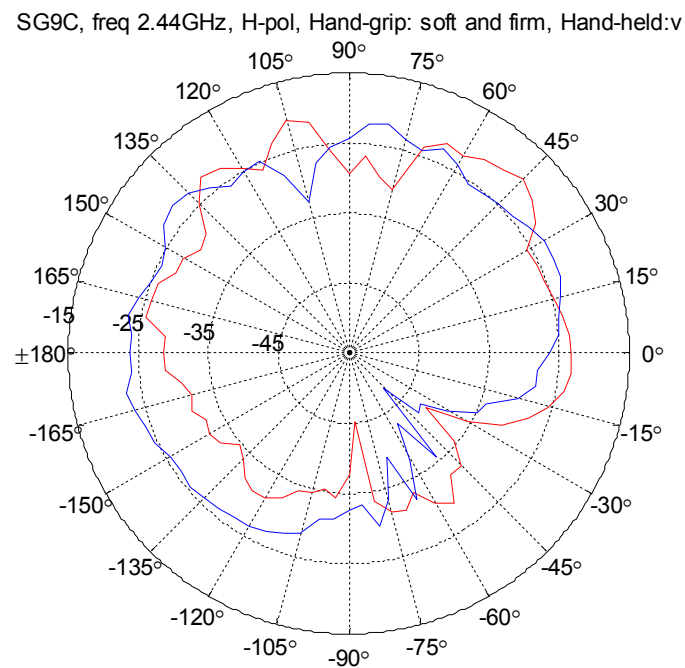


Figure 9 Measured gain in azimuth: soft-grip (blue), firm-grip (red)

Even though this result can be encouraging to extract conclusions of the hand grip effect and it's been shown in some studies that the user degrades the MEG, we can observe that if we look at the average difference between the mean effective gain (MEG) (for both hand-held positions, soft and firm respectively) for

the three portables used, that no conclusion can be observed.

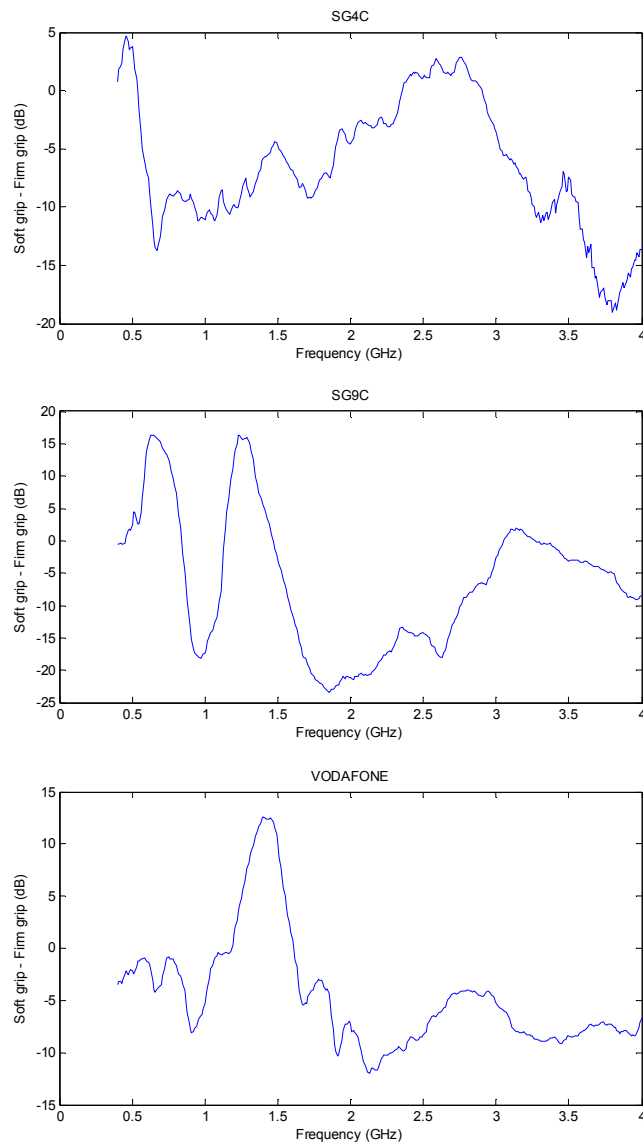


Figure 10 Gain difference (in dB) for Firm grip – Soft grip (SG4C, SG9C and Vodafone)

### 3.3 SAM head phantom

SAM - the Standard Anthropomorphic Model - is a head shell phantom intended primarily for use in the measurement of exposure from mobile phones (or other hand-held transmitters), but also eminently suitable for radio radiation pattern testing [18].

SAM was defined as standard phantom allowing a conservative measure of the radio exposure of people of all origins and all ages. The ear region was been

defined with reference points and planes to facilitate reproducible positioning of telecommunications devices.

SAM was originally developed as part of project SARSYS, a European Collaborative Research Programme under the EUREKA scheme. The SARSYS consortium members were MCL, SPEAG and the University of Ghent.

To guide the specification of a realistic shape phantom, the anatomical shape and size were obtained from the data of a large anthropometric study of men and women of various ethnic origins, aged over 20 years, randomly selected among US Army personnel. The study was carried out in the late 1980s; its findings are considered to be still representative of today's society. The dimensions of a 90th percentile male head were selected for the phantom.

CENELEC, IEC and IEEE have developed standard procedures for assessing exposures from mobile phones which specify the use of a SAM phantom. The Cellular Telecommunications & Internet Association (CTIA) has specified a phantom head, based on the SAM dataset, for the measurement of radiated RF Power and receiver performance.

### 3.3.1 Measurements

Measurements were performed with the following parameters:

Measurement equipment	VNA Rohde & Schwarz ZVA40
Band Width	400 MHz – 7 GHz
Frequency step	10 MHz (661 steps)
BW Resolution	1 KHz
Azimuth step	5° (69 steps)
Power	16 dBm
Terminal	Sagem SG9C
Orientation (respect ear to mouth)	-15°, 0°, +15°
Tilt	0°, +20°

This campaign provides us a total of 12 different phone positions and 661

frequency points for 69 different azimuth angles. The next figure shows what orientation and tilt angles mean:

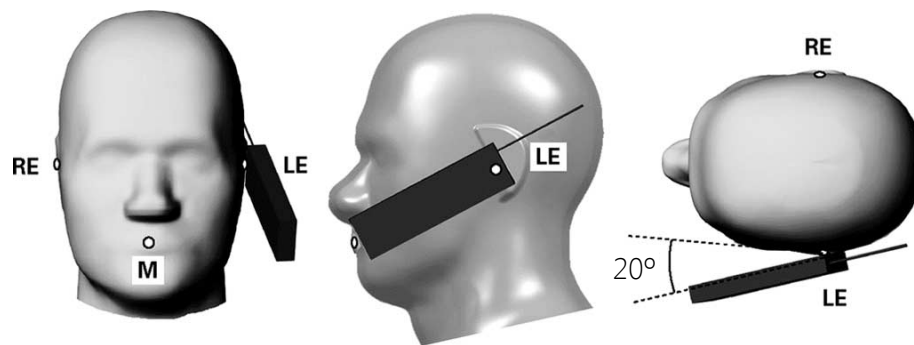


Figure 11 Orientation and tilt angles

Tilt is the angle that we can observe in the third figure. And orientation is the angle between the imaginary line ear-to-mouth and the vertical of the phone.

The scenario is described in the next figure. The rotation direction is clockwise. For  $\text{Theta}=+90^\circ$  the phone is in non-line-of-sight of the antenna.

Azimuth= $0^\circ$

Rotation direction (clockwise)

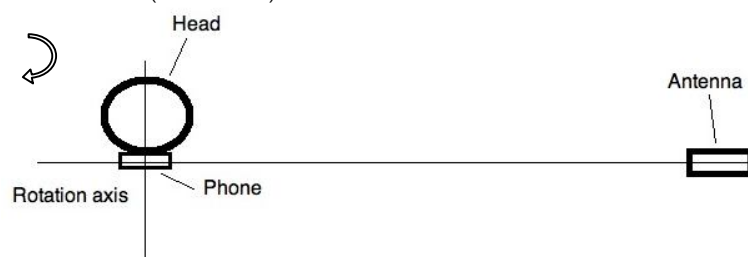


Figure 12 Schema of the scenario for Head phantom measurements

This is a photo of the actual scenario of the measurements:



Figure 13 Actual scenario for SAM head phantom measurements

The next figure is an example of the radiation pattern (measured gain in azimuth). This figure compare for a freq=2.44 GHz and orientation=0° the difference between tilt=0° (red) and tilt=20° (blue) for horizontal polarization:

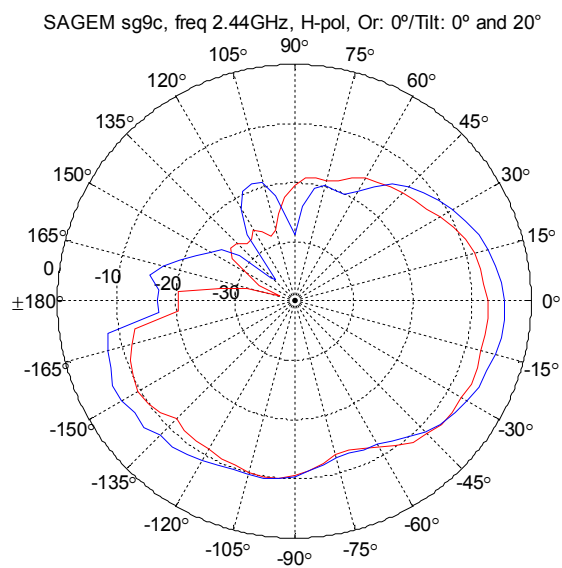


Figure 14 Measured gain in azimuth: tilt 0° (red), tilt 20° (blue)

The figure 14 show the differences between the different orientations for the previous measurement, setting the tilt at 0°. Different orientations are shown in the figures -15° (red), 0° (blue) and +15° (green)

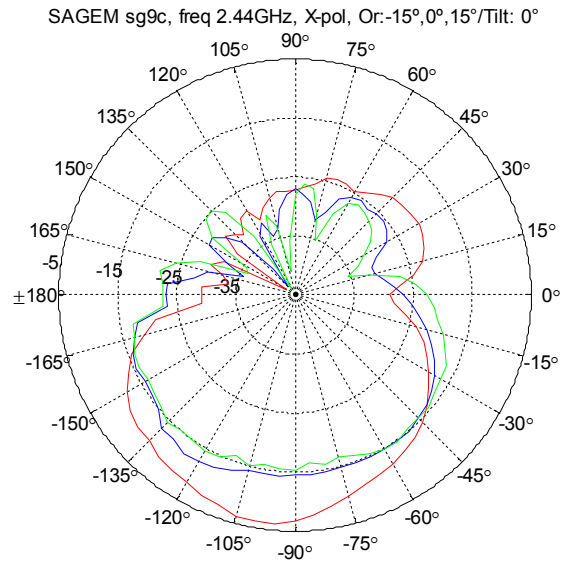


Figure 15 Measured gain in azimuth: orientation -15° (red), 0° (blue), 15° (green)

In both figures 13 and 14 we notice the very low radiation on the head side (positive angles) and a slight difference of radiation characteristics between different orientations and different tilts.



# Chapter 4. Design and manufacturing of new UWB devices

In choosing an antenna topology for UWB design, several factors must be taken into account including physical profile, compatibility, impedance bandwidth, radiation efficiency, directivity and radiation pattern. Several antennas were designed, simulated, fabricated, tested and characterized.

35

---

These antennas (see Appendix) are designed using CST Micro Wave Studio software. For running the simulations, the transient solver simulation tool is being used in CST software, which utilizes the staircase mesh and solves Maxwell's equations through a Finite Difference Time Domain technique called the "Leap-Frog algorithm".

## 4.1 Simulations

We will consider the antenna that reported the best results; the circular disc monopole array. This array antenna is designed based on the successful results obtained with the elemental antenna.

The elemental antenna was a Circular Disc Monopole [19], this monopole can be fed by a microstrip line. The circular monopole with a radius of  $r$  and a  $50\Omega$  microstrip feed line are printed on the same side of the substrate. The width of

the microstrip feed line is fixed to achieve  $50\Omega$  impedance. On the other side of the substrate the conducting ground plane only covers the section of the microstrip feed line.

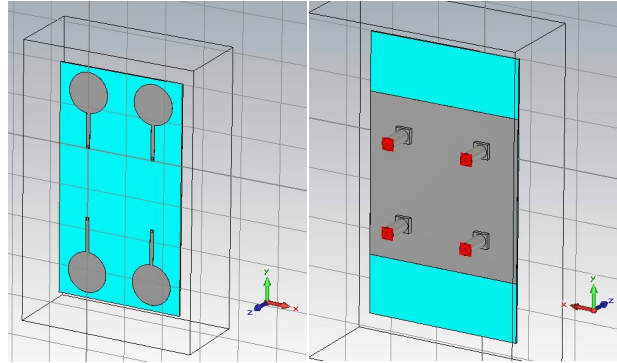


Figure 16 Frontal and back perspective views

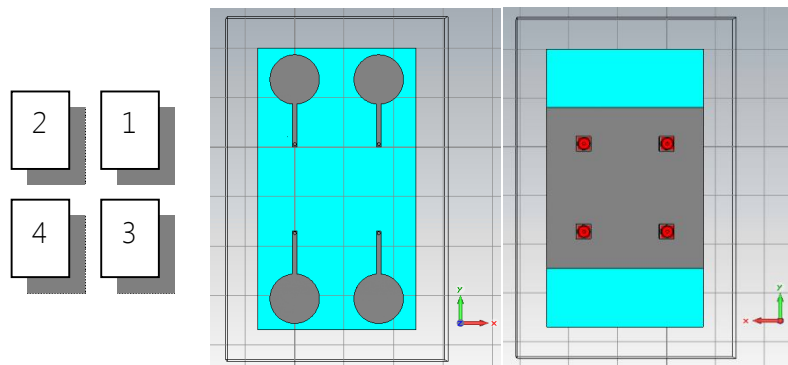


Figure 17 Ports distribution. Frontal and back views

In the next figures, we will show the results for S-parameters for the simulations in the 1 to 7GHz frequency band.

The first figure illustrates the simulated return loss curve,  $|S_{11}|$ , along the frequency band. The goal for the antenna is to be less than -10dB. The result is almost a complete frequency band under -10dB from 2.2GHz to 5.4GHz.

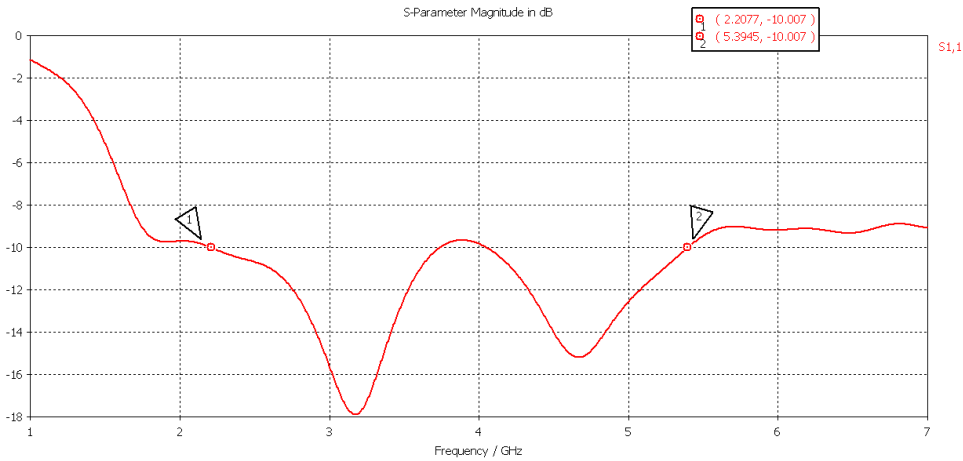


Figure 18  $|S_{11}|$  in dB for the multiport monopole circular antenna

It can be interesting to compare this result with the one obtained for the monoantenna monopole circular antenna showed in the next figure.

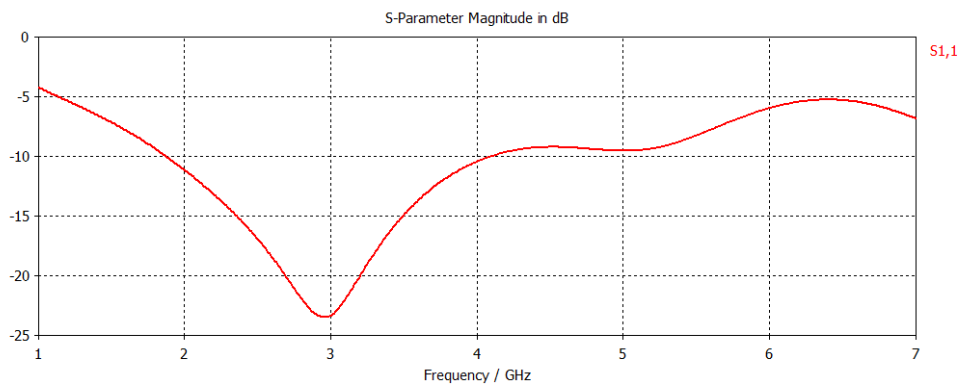


Figure 19  $|S_{11}|$  in dB for the monoport monopole circular antenna

As it is easy to notice the  $S_{11}$  has improved remarkably. This matching improvement especially for lower frequencies can be associated to the bigger size of ground plane.

The next 3 figures will show the coupling between the port 1 and the other 3 ports ( $|S_{21}|$ ,  $|S_{31}|$  and  $|S_{41}|$ ). These figures show the existing decoupling between the ports. It is easy to note that the best decoupling is between ports 1 and 4.

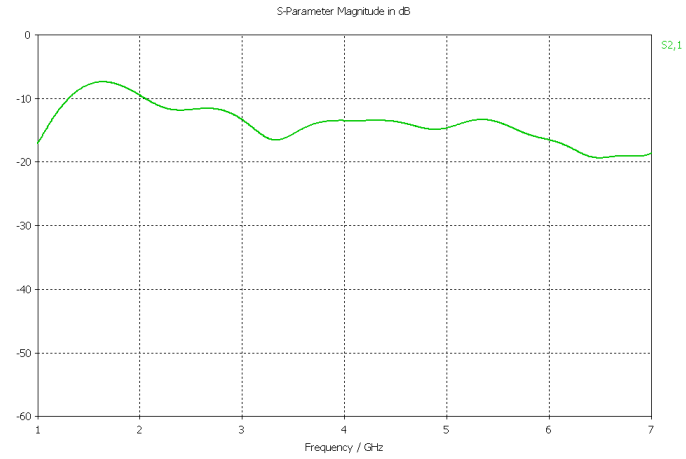


Figure 20  $|S_{21}|$  in dB for the monopole circular array antenna

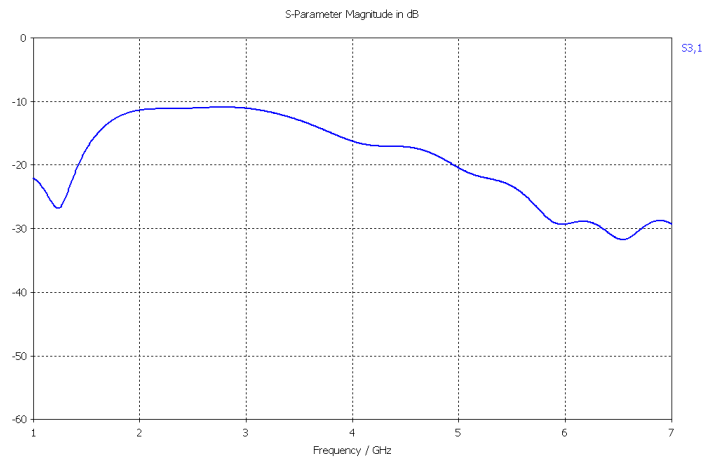


Figure 21  $|S_{31}|$  in dB for the monopole circular array antenna

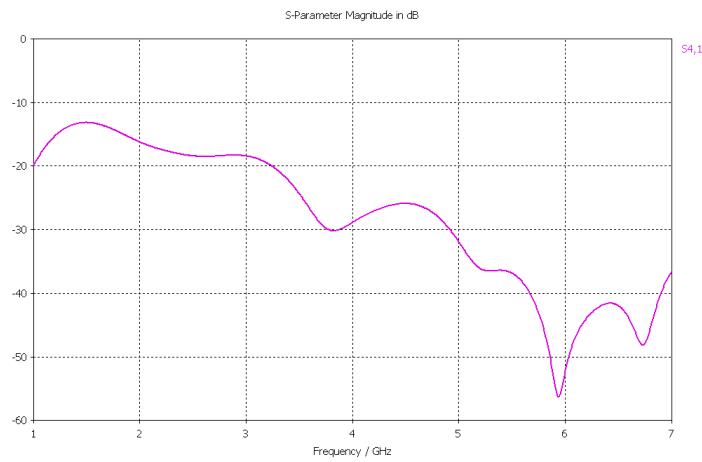


Figure 22  $|S_{41}|$  in dB for the monopole circular array antenna

These figures also show us how the decoupling effect is increased alongside the frequency. This makes completely sense since the higher is the frequency the smaller the wavelength and the bigger the electrical distance between ports.

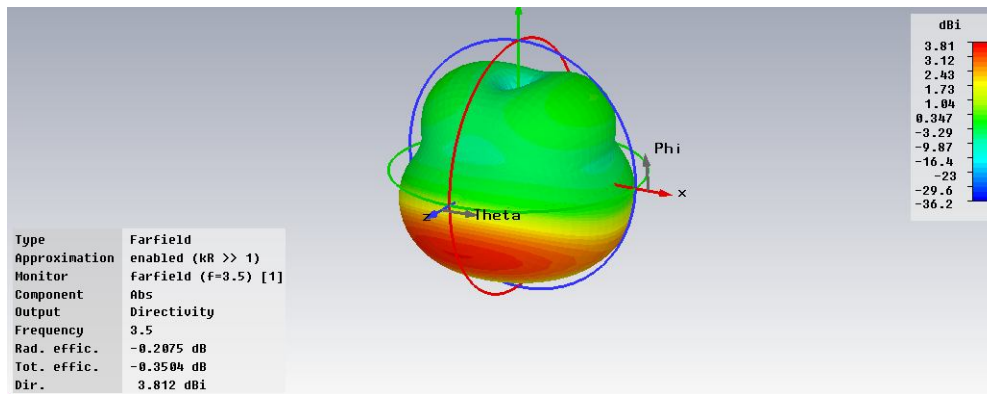


Figure 23 Radiation pattern for the monopole monopole circular antenna

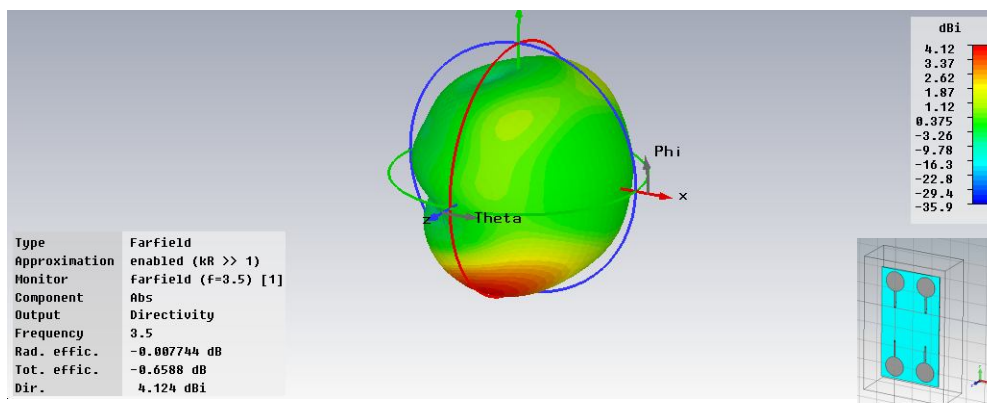


Figure 24 Radiation pattern for the monopole circular array antenna

Figures 22 and 23 compare the radiation patterns for the monopole (elemental) antenna and the array antenna for the frequency 3.5GHz. The simulated 3D radiation pattern plotted for the monopole antenna looks like a doughnut, similar to a dipole pattern as shown in figure 22. In figure 23, the radiation pattern of antenna 1 of the array antenna shows a difference with respect to the elemental antenna. It can be noted that the holes of the doughnut have almost disappeared. It is due to the bigger size of the terminal, specially the ground plane, and the influence of other radiating elements. Figures 24 and 25 show the cut for the angle  $\Theta = 90^\circ$ .

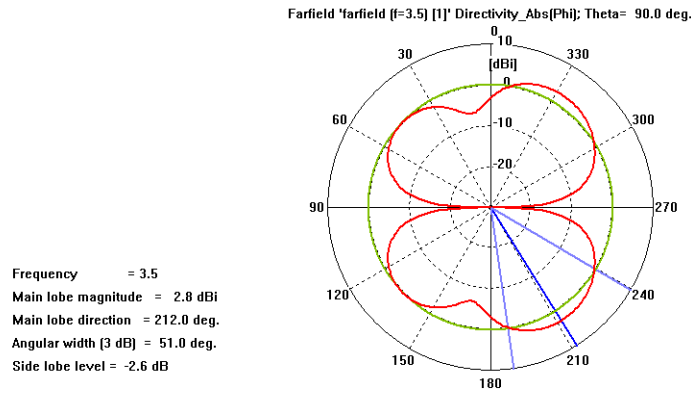


Figure 25

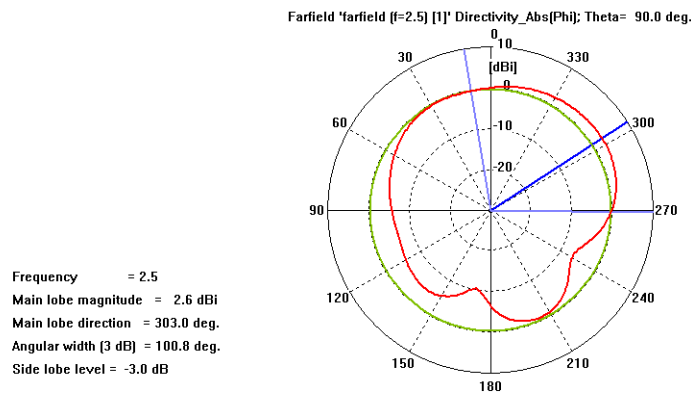


Figure 26

## 4.2 Measurements

In order to fabricate the antennas we used the software package LPKF CircuitCam and BoardMaster. CircuitCam software imports the design from Gerber files created by CST and allows the user to modify or change the layout. After this process the project file is sent to BoardMaster software. This program prepares layout files to send to LPKF circuit board plotter.

These are the specifications of the design for the circular monopole array antenna:

Height	114 mm
Width	64 mm
Diameter	20 mm
Line width	1.742 mm
Substrate thickness	0.762 mm

Copper thickness	0.035 mm
Relative permittivity	3.48 F/m

The following figures show the S parameters measured in the lab with the HP VNA. Some of the points are remarked for their importance:

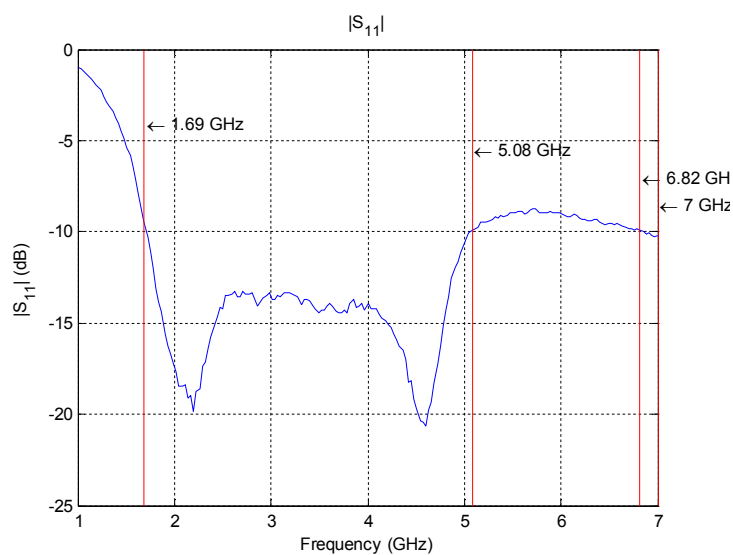


Figure 27  $|S_{11}|$  measured

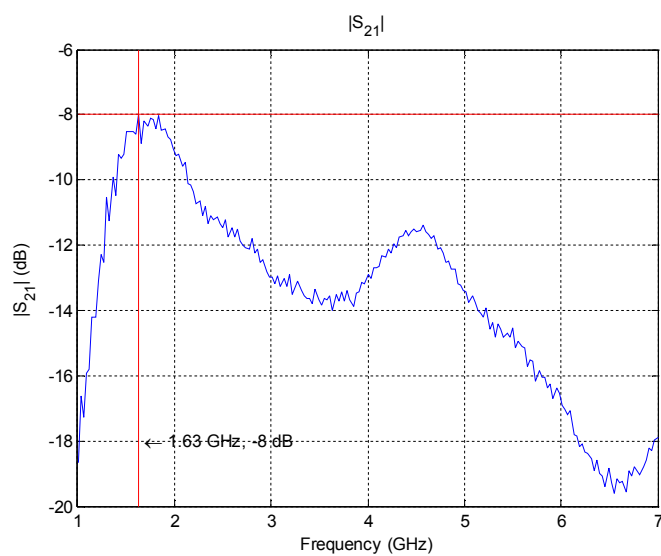


Figure 28  $|S_{12}|$  measured

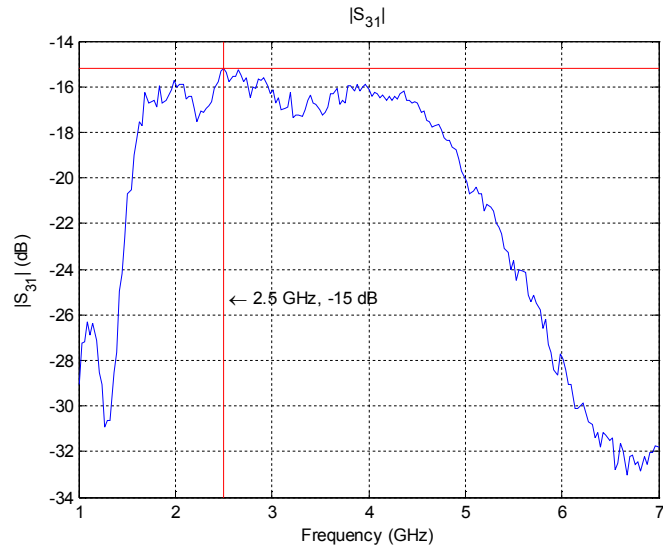


Figure 29  $|S_{13}|$  measured

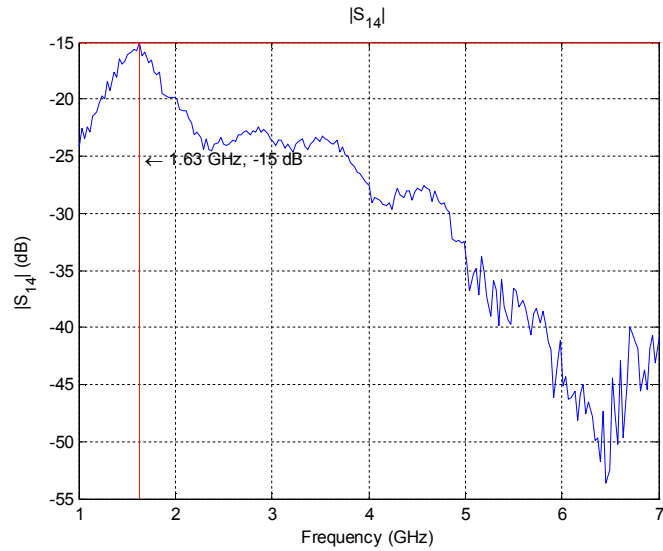


Figure 30  $|S_{14}|$  measured

These figures can be compared to the ones obtained in the CST simulations. As we noticed previously in other measurements the graphic is moved to the left, this means that the antenna is under the -10dB from 1.69GHz to 5.08GHz instead of the 2.2GHz-5.4GHz band that we obtained in the simulation.

The worst performance in the band 5GHz-7GHz does not disqualify the terminal since the maximum return loss in this band is -8dB. But attention must be taken about the high mutual coupling  $|S_{21}|$  for the band 1.76GHz – 2 GHz which accommodates important communication systems such as GSM and UMTS.



## 4.3 Conclusion

In this report, a comprehensive study of Multi antennas systems including design, simulation, testing and characterization is presented. Several parameters were taken into account in analyzing strengths and weaknesses in potential antenna designs including return loss, radiation pattern, directivity and mutual coupling.

Taking into account the tradeoffs of each antenna topology, the design that achieves the best result was the Circular Disc Monopole Array Antenna. The antenna covers many communication system bands (GSM, UMTS, WLAN and WiMAX) in a compact planar design, which is a difficult result to achieve.

Future work with regard to Multi antenna systems design should include packaging considerations, simulation and ground effects.



# Appendix

## ANTENNAS

Different antennas designs were carried on. The next figures will show them and the results achieved on CST simulations. Some of them were just designed and rejected due to unsuccessful results.

### FRACTUS

This array antenna is designed taking into account the use of multiples Fractus® Compact Dual-band Reach Xtend™ Chip Antenna.

The Fractus Compact Dual-band Reach Xtend Chip Antenna for 802.11 a/b/g/n WLAN systems is a tiny rectangular 3D-shaped antenna specifically designed for high performance USB devices and other small PCB devices operating at both 2.4 GHz and 5 GHz bands, where high performance and low-cost are mandatory. Its small dimensions allow various configurations within the USB devices and may help Cardbus devices in the enhancement of their throughput by using MIMO algorithms with more than 2 antennas (Fractus).



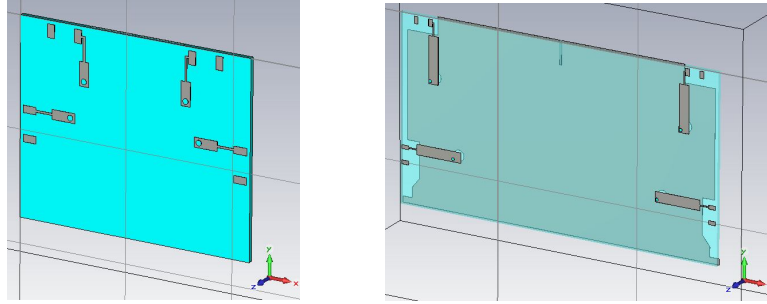


Figure A. 1 (a) Fractus I and (b) Fractus II.

## ANTENNOVA

This array antenna is designed taking into account the use of multiples antennas Flavus Penta-band: p/n B5812-xx.

Flavus Penta-band is a low profile snap-in antenna. It is intended for applications which demand both a very high performance antenna,



but also easy assembly directly onto the printed circuit board. Flavus is snapped onto the PCB by hooks and is available in a series of dimensions that meets various PCB thicknesses.

Flavus is available in different frequencies and has been implemented in units like wireless access point, printers, etc, but other application areas might be just as applicable (Antenna).

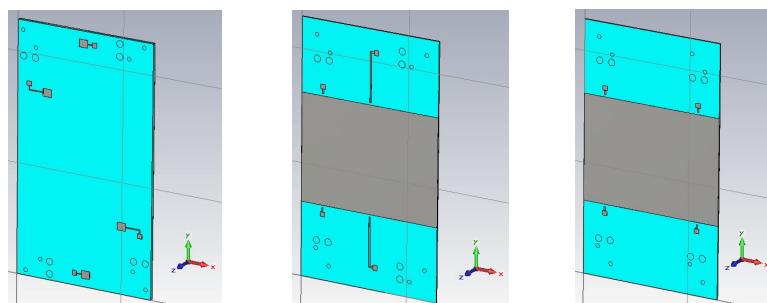


Figure A. 2 (a) Antenna I, (b) Antenna II and (c) Antenna III.

## SLOT ANTENNA

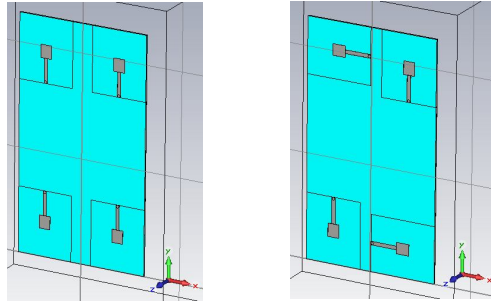


Figure A. 3 (a) Patch and (b) Patch 90

A Design about planar microstrip-line-fed slot antenna utilizing a simply L-shape slot for bandwidth enhancement is investigated, printed and measured. By selecting a suitable ratio of its axes, it can be found that the ultra-wideband operation can be obtained.

## PIFA ANTENNA

We also realized measurements of a PIFA (Planar Inverted F Antenna) antenna provided by the Université of Limoges through collaboration with Professor Alain Sibille.

PIFA antenna typically consists of a rectangular planar element located above a ground plane, a short circuiting plate or pin, and a feeding mechanism for the planar element (Rosu).

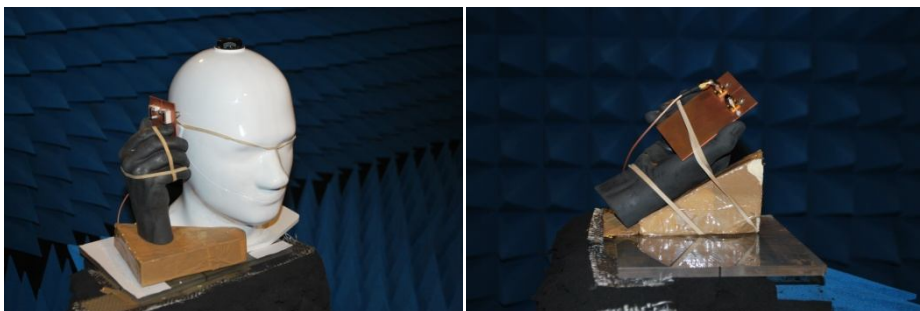
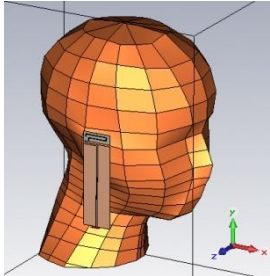
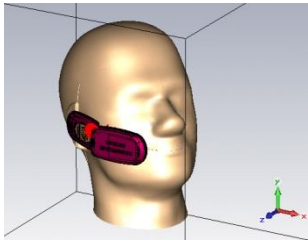
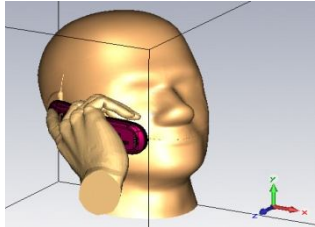
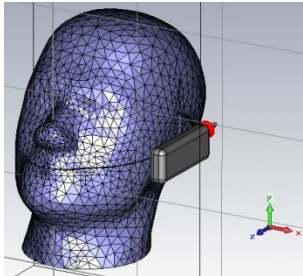
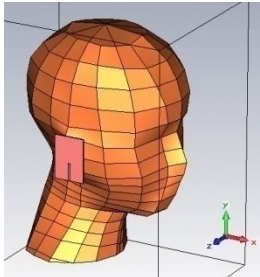
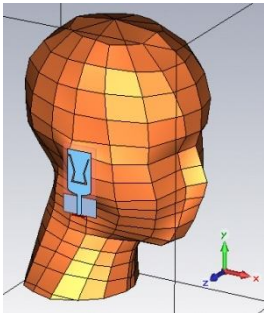


Figure A. 4 Scenario for (a) Head measurements and (b) PDA measurements

This measurement campaign was carried out with the same goal as the previous measurements; collect statistical variability by varying the position of the terminal plus phantom (both hand and head).

# SIMULATIONS

Several simulations were carried on following the work of PhD student Amine Mellah.

Biband	Total of simulations 30		
	Parameters	rotation distance tilt	
Clapet (tete)	Total of simulations 25		
	Parameters	rotation tilt	
Clapet (tete_main)	Total of simulations 15		
	Parameters	rotation tilt	
Helix	Total of simulations 15		
	Parameters	rotation tilt	
MDIS(uwb)	Total of simulations 30		
	Parameters	rotation tilt distance	
MLTB	Total of simulations 30		
	Parameters	rotation tilt distance	

# Bibliography

[1] Braga, J., "Sondage de canal SIMO à l'intérieur des bâtiments et formation de faisceaux numérique utilisant des techniques de traitement de signal à haute résolution et corrélateurs cinq-ports, " PhD Thesis, 2006

[2] Balanis, C., "Modern Antenna Handbook," JOHN WILEY & SONS. September 2008.

[3] Chen, Z. N., "Antennas for portable devices," Singapore: John Wiley & Sons. 1<sup>st</sup> Edition. March 2007

[4] Clarke, Karunaratne, & Schrader, "Ultra-Wideband Antenna," *EE198B*. 2004.

[5] Berenguer, Adeane, Wassell, & Wang, "Lattice-Reduction-Aided Receivers for MIMO-OFDM in spatial multiplexing systems," *IEEE PIMRC 2004*, Barcelona, Spain, Sep. 2004.

[6] Chiau, Chen and C.G.Parini, "A Sandwiched Multi-period E B G Structure for Microstrip Patch Antennas," *Microwave and Optical Technology Letter*, vol. 46, no. 5, pp. 437-440, 5 September 2005.

[7] Plicanic, and Z. Ying, "Two-antenna receive diversity performance in indoor environment," *Electronics Letters* vol. 41, n°22, pp. 1205-1206. 2005.

[8] Sibille, A., & Mellah, A, "Urban planning for Radio Communications," 2nd Version. 2008.

[9] Barroso, M.J. Rendas, and J.P. Gomes, "Impact of array processing

techniques on the design of mobile communication systems," *7th IEEE Mediterranean Electrotechnical Conference*, vol. 3, pp. 1291-1294, Antalya, Turkey, April 1994.

[10] M. Beach, M. Hunukumbure, C. Williams, et al., "An experimental evaluation of three candidate MIMO array designs for PDA devices," *COST 273/284 Workshop on Antennas and Related System Aspects in Wireless Communications, Gothenburg, Sweden*, June 2004.

[11] F. Harrysson, J. Medbo, A. F. Molisch, A. Johansson, and F. Tufvesson, "The composite channel method: Efficient experimental evaluation of a realistic MIMO terminal in the presence of a human body," *IEEE Veh. Technol. Conf. (VTC'08-Spring)* pp. 473-477. May 2008.

[12] Milligan, T., "Modern Antenna Design," JOHN WILEY & SONS. 2nd Edition. New Jersey, July 2005.

[13] Sibille, A., & Roblin, C., "Antennes intégrées et microstructurées".

[14] Carr, J., "Practical Antenna Handbook," *McGraw Hill*. 4th Revised edition. May 2001.

[15] Plicanic, V., Lau, B. K., & Ying, Z., "Performance of a Multiband Diversity Antenna with Hand Effects," *IEEE Transactions on Antennas and Propagation*, Vol. 57, No. 5, pp. 1547-1556, 2009.

[16] K. Ogawa, T. Matsuyoshi and K. Monma, "An analysis of the performance of a handset diversity antenna influenced by head, hand, and shoulder effects at 900 MHz:Part II - Correlation characteristics," *IEEE Trans. on Vehicular Technology*, vol. 50, no.3, pp. 845-853, May 2001.

[17] K. Meksamoot, M. Krairiksh and J. Takada, "A polarization diversity PIFA on portable telephone and human body effects on its performance," *IEICE Trans. Commun.*, vol. E84-B, no. 9, Sep. 2001.



[18] C. Gabriel, "Tissue equivalent material for hand phantoms," *MCL-t*, London, UK. 2007.

[19] B. Allen, M. Dohler, E.E. Okon, W.Q. Malik, A.K. Brown, D.J. Edwards, Editors, "Ultra Wideband Antennas and Propagation for Communications, Radar and Imaging," JOHN WILEY & SONS. 2007

[20] M. Pelosi, G.F. Pedersen and M.B. Knudsen, "Investigation of the hand grip positions of mobile phone users: experimental campaign outline," *COST 2100 TD(07) 320*, Duisburg, Germany, 10-12 Sept. 2007.

[21] K. C. Lee, J. Y. Jhang, and M. C. Huang, "Performance of underwater adaptive array including mutual coupling effects," National Cheng-Kung University, Taiwan, 2007.

[22] Keith B. Schaub, Joe Kelly, "Production testing of RF and system-on-a-chip devices for wireless communications," 2004.